



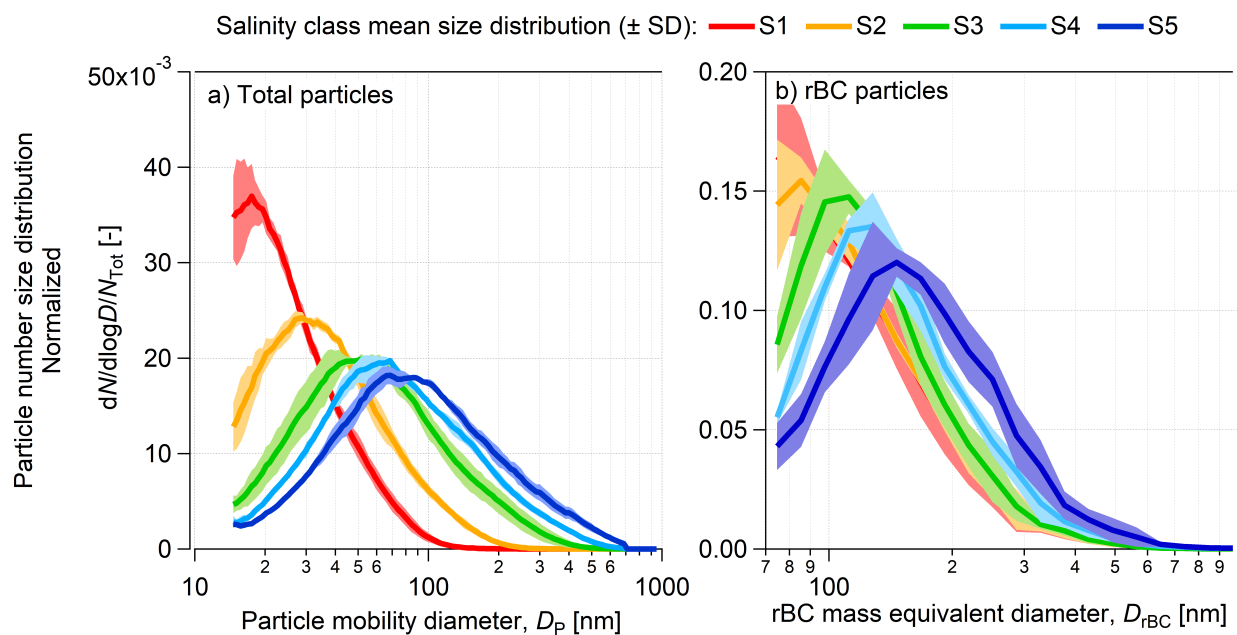
Supplement of

Technical note: Sea salt interference with black carbon quantification in snow samples using the single particle soot photometer

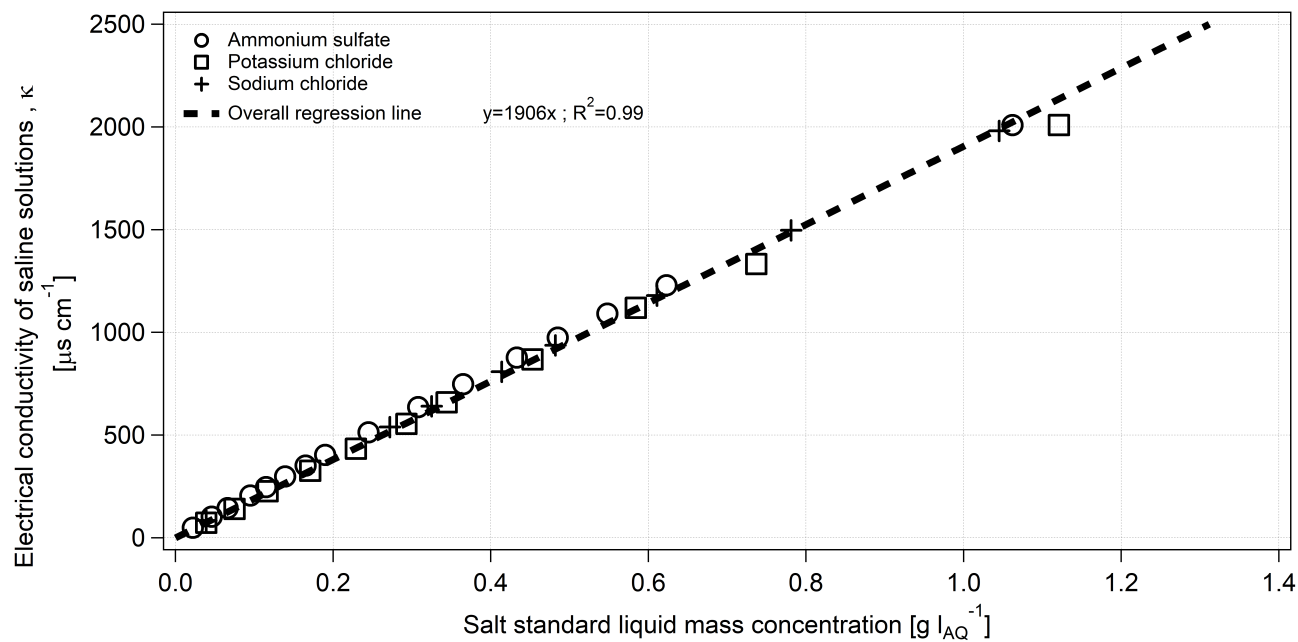
Marco Zanatta et al.

Correspondence to: Andreas Herber (andreas.herber@awi.de)

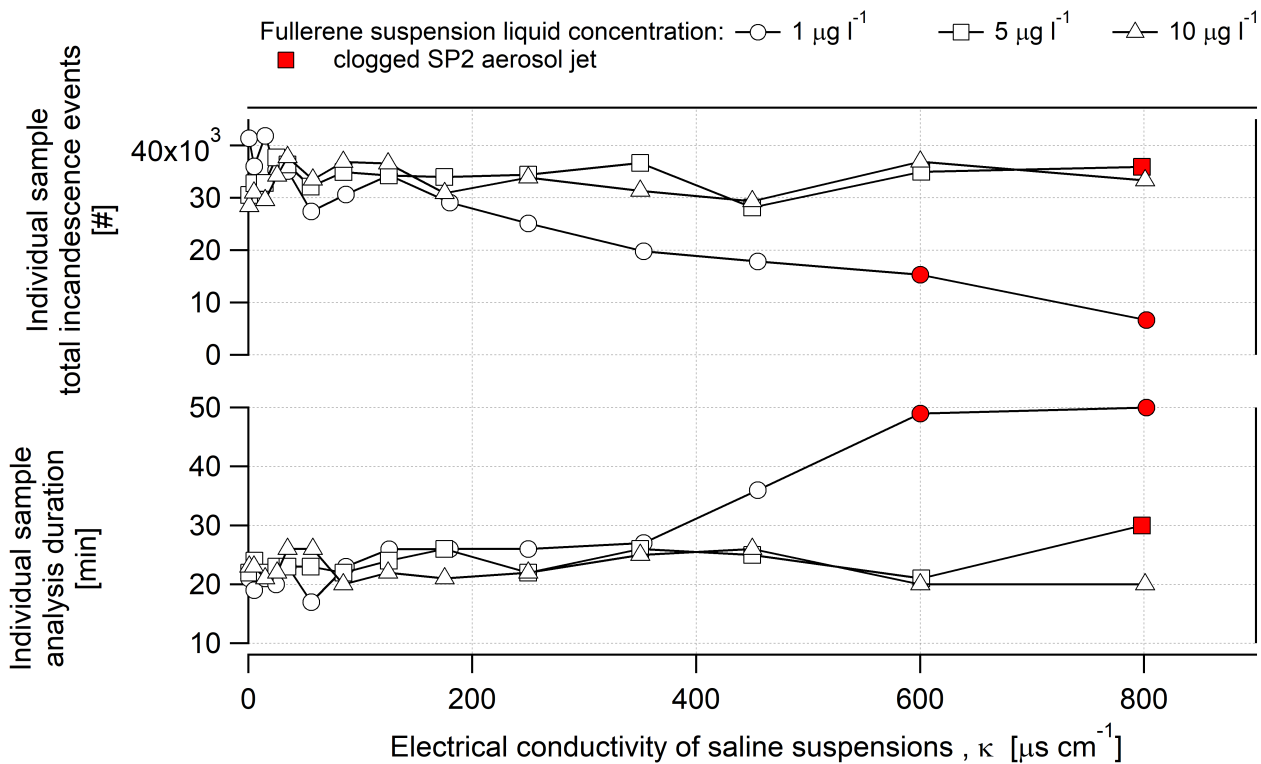
The copyright of individual parts of the supplement might differ from the article licence.



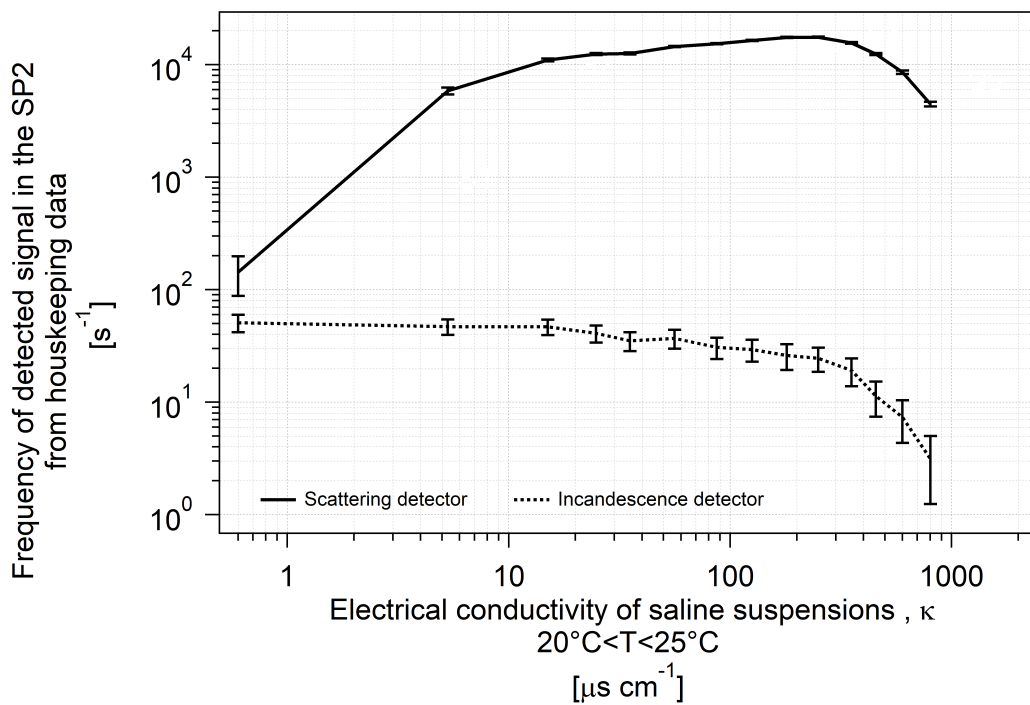
5 **Figure S1** Normalized size distribution of total (a) and rBC particles (b) aerosolized from PASCAL snow samples grouped in salinity classes. Total particles measured with the SPMS in the 14-680 nm diameter range nm. rBC particles measure with the SP2 in the 70-1000 nm diameter range.



10 Figure S2 Electrical conductivity of saline solutions as a function of salt liquid mass concentration. Electrical conductivity measured between 22 and 23°C.

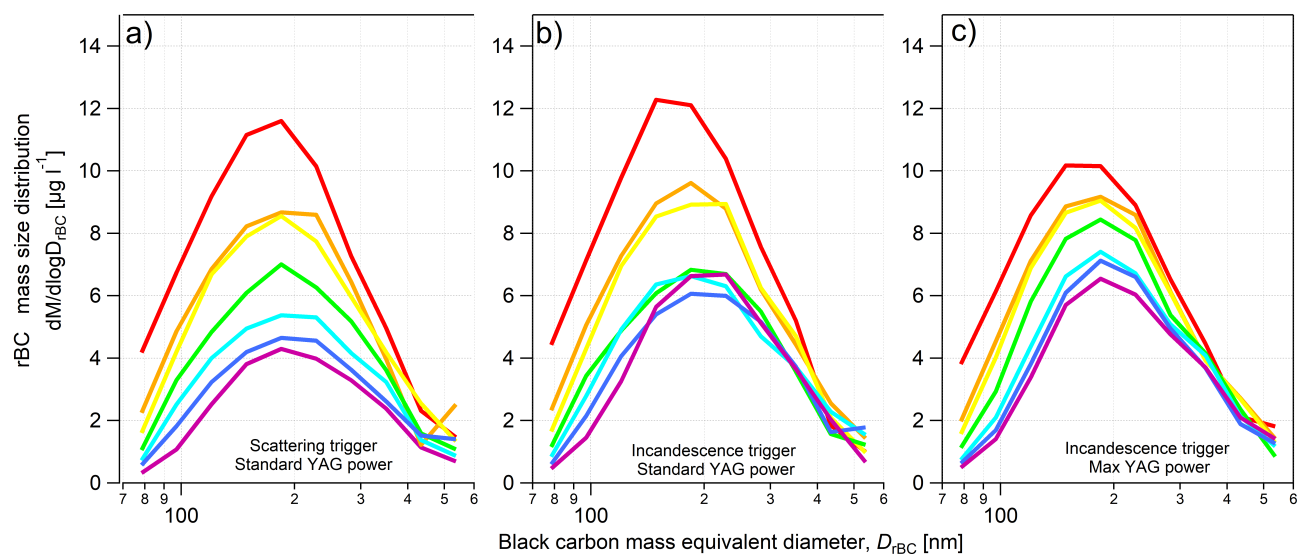


15 Figure S3 Total incandescence events and analysis duration of fullerene soot suspensions at different concentration and in increasing electrical conductivity.



20 **Figure S4** Frequency of detected scattering and incandescence signal in the SP2 recorded in the housekeeping data during the analysis of fullerene soot suspension (10 μg l⁻¹) with increasing NaCl concentration. Signal acquisition triggered over the scattering detector.

Electrical conductivity of fullerene suspension, κ [$\mu\text{s cm}^{-1}$]: — 0 — 50 — 100 — 200 — 400 — 600 — 800
 Fullerene suspension mass concentration: $10 \mu\text{g l}^{-1}$



25

Figure S5 rBC mass size distribution for different SP2 settings. a) acquisition triggered on the scattering detector with standard YAG-laser output power, $\epsilon_{\text{SP2-Tin}}$; b) acquisition triggered on the incandescence detector with standard YAG-laser output power $\epsilon_{\text{SP2-Tin}}$; c) acquisition triggered on the incandescence detector with maximum YAG-laser output power, $\epsilon_{\text{SP2-Tin,max}}$. Results for fullerene soot suspensions with a concentration of $10 \mu\text{g l}^{-1}$.

30

Table S1 Theoretical coating thickness of BC particles suspended from saline suspensions at increasing electrical conductivity (κ) calculated assuming: concentric core-shell geometry, single BC particle-containing droplet, droplet diameter (D_o) of 5 μm , 8 μm and 12 μm .

κ [$\mu\text{S cm}^{-1}$]	Coating thickness [nm]														
	D_{nc} 100 nm			D_{nc} 200 nm			D_{nc} 300 nm			D_{nc} 400 nm			D_{nc} 500 nm		
	D_o 5 μm	D_o 8 μm	D_o 12 μm	D_o 5 μm	D_o 8 μm	D_o 12 μm	D_o 5 μm	D_o 8 μm	D_o 12 μm	D_o 5 μm	D_o 8 μm	D_o 12 μm	D_o 5 μm	D_o 8 μm	D_o 12 μm
0	0	0	0	0	0	0	0	0	0	0	0	0	0	0	0
50	18	47	90	6	21	54	3	11	32	2	6	20	1	4	13
100	30	69	125	11	37	84	5	20	55	3	12	37	2	8	25
200	46	98	170	21	60	126	10	36	90	6	23	64	4	16	47
400	68	135	226	36	93	180	20	62	140	12	42	107	8	30	82
600	84	161	266	49	118	219	28	83	177	17	59	141	12	42	111
800	97	182	298	59	138	250	36	101	207	23	73	168	15	54	136

35

Table S2 Theoretical coating-rBC mass ratio of BC particles suspended from saline suspensions at increasing electrical conductivity (κ) calculated assuming: concentric core-shell geometry, single BC particle-containing droplet, droplet diameter (D_o) of 5 μm , 8 μm and 12 μm .

κ [$\mu\text{S cm}^{-1}$]	Coating-rBC mass ratio [nm]														
	D_{nc} 100 nm			D_{nc} 200 nm			D_{nc} 300 nm			D_{nc} 400 nm			D_{nc} 500 nm		
	D_o 5 μm	D_o 8 μm	D_o 12 μm	D_o 5 μm	D_o 8 μm	D_o 12 μm	D_o 5 μm	D_o 8 μm	D_o 12 μm	D_o 5 μm	D_o 8 μm	D_o 12 μm	D_o 5 μm	D_o 8 μm	D_o 12 μm
0	0.00	0.00	0.00	0.00	0.00	0.00	0.00	0.00	0.00	0.00	0.00	0.00	0.00	0.00	0.00
50	1.81	7.43	25.1	0.23	0.93	3.14	0.07	0.27	0.92	0.03	0.12	0.39	0.01	0.06	0.20
100	3.63	14.9	50.1	0.45	1.86	6.28	0.13	0.55	1.85	0.06	0.23	0.79	0.03	0.12	0.40
200	7.26	29.7	100	0.91	3.72	12.6	0.27	1.09	3.69	0.11	0.47	1.57	0.06	0.24	0.81
400	14.5	59.4	201	1.82	7.45	25.1	0.53	2.19	7.38	0.23	0.93	3.15	0.12	0.48	1.62
600	21.8	89.2	301	2.73	11.2	37.7	0.80	3.28	11.1	0.34	1.40	4.72	0.18	0.72	2.42
800	29.0	119	401	3.64	14.9	50.3	1.07	4.38	14.8	0.46	1.87	6.29	0.23	0.96	3.23

40